Comparison of Different Modulations Strategies Applied to a Multilevel Flying Capacitor Inverter

Thiago Lazzari, Edivan Laercio Carvalho, Leandro Michels, Rodrigo Padilha Vieira, Humberto Pinheiro

Universidade Federal de Santa Maria – UFSM, Santa Maria - RS, Brazil
E-mails: thiago.lazzari@hotmail.com, edivan.labensaios@gepoc.ufsm.br, rodrigovie@gmail.com, michels@gepoc.ufsm.br, humberto.ctlab.ufsm.br@gmail.com

***Abstract*— This paper presents a comparison of different carrier-based modulation strategies. The modulation by geometric approach stands out due to the possibility of evenly distribution of the switching pulses between the semiconductors and reducing the harmonic distortions in the output voltage of DC-AC multilevel converters. The research presents possibilities to explore the degrees of freedom of this modulation in order to reduce the number of switching of the semiconductors, harmonic distortions, and regulate the voltage of the flying capacitors in a three-phase Flying Capacitor inverter. Comparisons with the carrier-based Discontinuous Modulation, Phase-Disposition, and Phase-Shift modulations with open loop are performed using simulation results obtained by the software PSIM.**

***Key-Words*— Flying Capacitor, Discontinuous Modulation, Multilevel Converters, Phase-Disposition Modulation, Phase-Shift Modulation.**

I. INTRODUCTION

Multivel inverters have been widely studied in applications such as photovoltaic and wind power generation systems, mainly because of the higher levels of current and voltage in high power stations [1]-[3]. In this type of application, semiconductors suffer greater demands. There is also a need to increase the quality of energy processing between generation sources and distribution systems [1].

For these situations, multilevel DC-AC converters, or multilevel inverters, are interesting because they operate with high voltage levels and low harmonics distortions using medium or low power semiconductors, for example, topologies like Flying Capacitor (FC) [3]-[4], Neutral Point Clamped (NPC) [5], or Interleaved Inverters [1], [6].

In addition to the aforementioned advantages, applications with appropriate modulation techniques allow to reduce harmonic distortions of output current, the switching number of semiconductors, as well as to explore specific points, like the control of the circulating current between parallel legs on Interleaved Inverters [1] or the voltage regulation of the flying capacitors [4].

There are different modulation techniques applied to multilevel inverters, like Space Vector modulation [7], [8], carrier-based modulations, such as Phase-Shift (PS) [9], [10], Phase-Disposition (PD) [12], and modulations with geometric approaches [1], [4], [13].

Among these modulation techniques, modulations with geometric approaches stands out because they offer advantages in relation to higher degrees of freedom, which can be used for different purposes, for example [1], [4], [13]:

i) Uniform distribution of switching between semiconductors;
ii) Minimization of the harmonic distortion of the output current;
iii) Reduction of switching losses;
iv) Increase the capacity of the inverter to synthesize sinusoidal voltages.

A carrier-based Discontinuous Modulation (DM) is presented in [1], which proposes a modulation strategy that alternates between points that representing – within a linear operating region – the maximum and minimum values of the common mode voltage of an Interleaved Inverter. As a result, multilevel line voltage with low harmonic distortions are presented, as well the control of the circulating current between the parallel legs of the inverter.

These degrees of freedom were used in [4] in order to regulate the voltages of the flying capacitors in a three-phase FC inverter. In this paper, the same topology of a three-phase FC inverter is adopted, which is shown in Figure 1. However, this paper differs from [1] and [4] by extending the analyzes of the carrier-based DM, comparing this strategy with others of interest, such as PD and PS modulations during the steady state operation.

The PD modulation has a reduced harmonic distortion compared to PS modulation, however presents a disadvantage in relation to the switching of its semiconductors. Despite of the number of switching is reduced, the switching frequency of the semiconductors is high during a part of time and during the other part, the switching frequency of the semiconductors is clamped. On the other hand, the PS modulation has a greater number of commutations, but distributed evenly over time. Thus, the carrier-based DM comes with the purpose to joining advantages of both PD and PS modulations, with the aim of achieving a small number of commutations compared to PS modulation, but with a uniform distribution of theses commutations when compared to PD modulation [1], [9]-[12].

The development and analysis of converter and modulations are presented in this paper, organized as follow: section (II) shows the modulations of interest, with emphasis on the carrier-based DM; in (III) the simulation results are obtained as well the discussion of these results. Finally, section (IV) presents the conclusions of this paper.

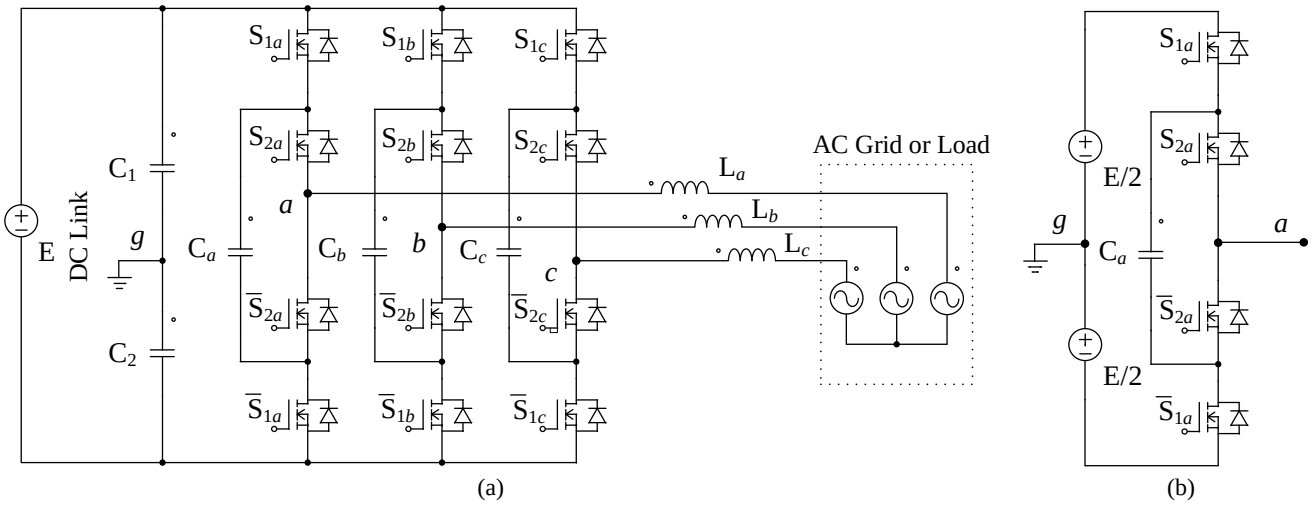

Fig. 1. a) Power circuit of Flying Capacitor converter; b) equivalent circuit of phase *a*.

II. CARRIER-BASED MODULATIONS

The PD and PS modulations present features that motivate the development of carrier-based DM, which combines advantages of both modulations. The methods of implementing of the PD, PS and DM modulations will be shown in the following subsections. The modulating signal V_{x_eq}, used for analysis are represented by:

$$V_{x\_eq} = \frac{1}{2} + \frac{m_a \sin(\omega \cdot t + \theta)}{2}, \quad (1)$$

where x is a index of phases a, b, and c, m_a is the modulation index, ω is the angular frequency, and θ is the phase angle.

A. *Phase-Disposition (PD)*

The PD modulation, initially proposed in [14], compare a modulating signal with carriers shifted in amplitude. The number of carrier signals depends on the number of inverter levels, for example, in a three-level converter are used two carrier signals (C_1 e C_2) and one modulating signal (V_{x_eq}), as shown by Figure 2.

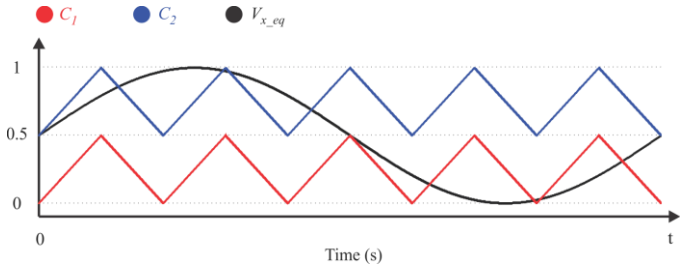

Fig. 2. Modulating signal and carriers for the implementation of PD modulation in three-level converter.

In general, the number of carriers is determined by m-1, where m is the number of levels of the converter [14]-[15].

B. *Phase-Shift (PS)*

Differently from the PD modulation that has the carriers shifted in amplitude, the modulation PS presents its carriers shifted to each other in 360/(m-1)°, where m is the number of levels of the inverter [15]. For example, a converter with three-levels could be modulated from two carriers signals (C_1 e C_2) shifted to each other in 180° and a modulating signal (V_{x_eq}), as illustrated in Figure 3.

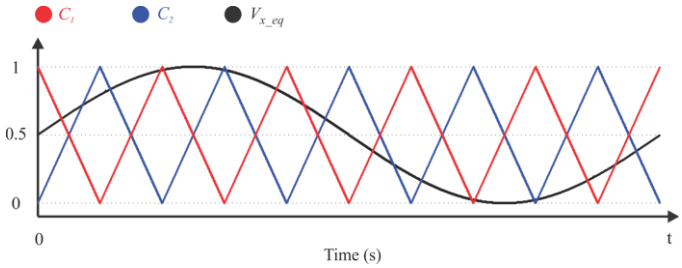

Fig. 3. Modulating signal and carriers for the implementation of PS modulation in a three-level converter.

C. *Carrier-Based Discontinuous modulation (DM)*

As well as the PD and PS modulations, the carrier-based DM also performs a comparison among modulating and carrier signals. However, in DM modulation only one carrier is used, while two modulating signals constitute a single equivalent signal. In addition, DM modulation is developed in the space of the converter phase voltages, while PD and PS modulations are developed from the converter line voltages [1], [4].

Thus, to generate the modulating signals of the FC converter presented in Figure 1-a, the mathematical analysis of phase *a* from Figure 1-b will be developed, which can be extended to the analysis for the others phases.

Considering the equivalent voltage (1) applied to phase *a*, as well the differential mode voltage V_{a_d}, – indicated in Figure 1-b –, both voltages can be represented in terms of V_{ag1} and V_{ag2}, given by:

$$V_{a\_eq} = \frac{V_{ag1} + V_{ag2}}{2}, \quad (2)$$

$$V_{a\_d} = V_{ag1} + V_{ag2}. \quad (3)$$

Rewriting (2) and (3) as a function of V_{x_eq} and V_{a_d}, V_{ag1} and

V_{ag2} can be represented as:

$$V_{ag1} = V_{a\_eq} + \frac{V_{a\_d}}{2}, \tag{4}$$

$$V_{ag2} = V_{a\_eq} - \frac{V_{a\_d}}{2}. \tag{5}$$

For the converter operating on a linear region, V_{ag1} and V_{ag2}, must satisfy the following inequalities:

$$0 \le V_{ag1} \le 1, \tag{6}$$

$$0 \le V_{ag2} \le 1. \tag{7}$$

Substituting (4) and (5) into (6) and (7) respectively, the following restrictions (R_1, R_2, R_3, R_4) must be met:

$$V_{a\_d} \le 2 - 2 \cdot V_{a\_eq} \rightarrow R_1 \text{ to } V_{a\_eq} \le 0.5, \tag{8}$$

$$V_{a\_d} \ge -2 + 2 \cdot V_{a\_eq} \rightarrow R_2 \text{ to } V_{a\_eq} \le 0.5, \tag{9}$$

$$V_{a\_d} \ge -2 \cdot V_{a\_eq} \rightarrow R_3 \text{ to } V_{a\_eq} > 0.5, \tag{10}$$

$$V_{a\_d} \ge 2 \cdot V_{a\_eq} \rightarrow R_4 \text{ to } V_{a\_eq} > 0.5. \tag{11}$$

Therefore, V_{a_d} must be defined in such a way as to meet the restrictions (8)-(10), so:

$$V_{a\_d} \ge \max(R_2, R_3), \tag{12}$$

$$V_{a\_d} \le \min(R_1, R_4). \tag{13}$$

In order to obtain a discontinuous modulation, the modulating signal is divided in two sectors: a) Sector 1 - when the modulating voltages are greater than 0.5 and V_{a_d} satisfies the restrictions R_1 and R_2; b) Sector 2 - when the modulating voltages are less than or equal to 0.5 and V_{a_d} satisfies the restrictions R_3 and R_4.

Figure 4 shows the modulating signals for maximum and minimum values of voltage V_{a_d} and the influence of these signals on the current behavior in the capacitor C_a of Figure 1.

In Figures 4-a and 4-b it is observed that both signals present a discontinuous behavior, where one of the signals saturates at the maximum or minimum value, while the other acts with a PWM modulation. In addition, it is possible to verify that the current behavior in the capacitor C_a is complementary to the choice of V_{a_d}. Thus, in order to make the average current in the capacitor zero and maintain the voltage in the capacitor naturally balanced, when using passive loads, it is possible to switch between the maximum and minimum limits of V_{a_d}, as shown in Figure 5. In addition, if the initial voltage in the capacitors are different from $V_{cc}/2$, the voltages will naturally reach the balance when the converter are applied to passive loads, even without a close loop control.

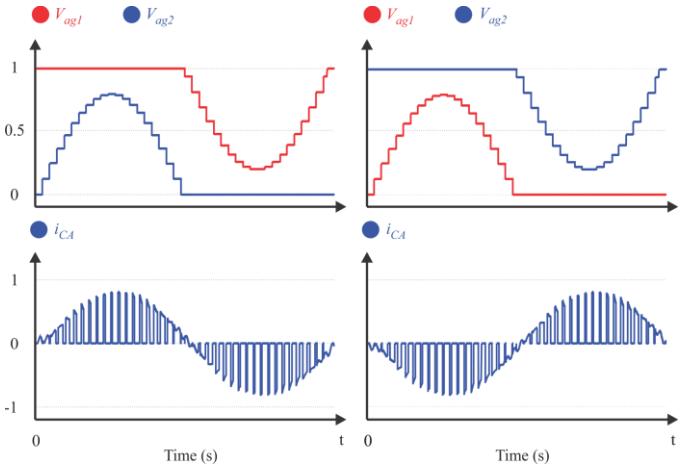

Fig. 4. a) Modulating signals using minimum values of V_{a_d} ;b) Modulating signals using maximum values of V_{a_d}.

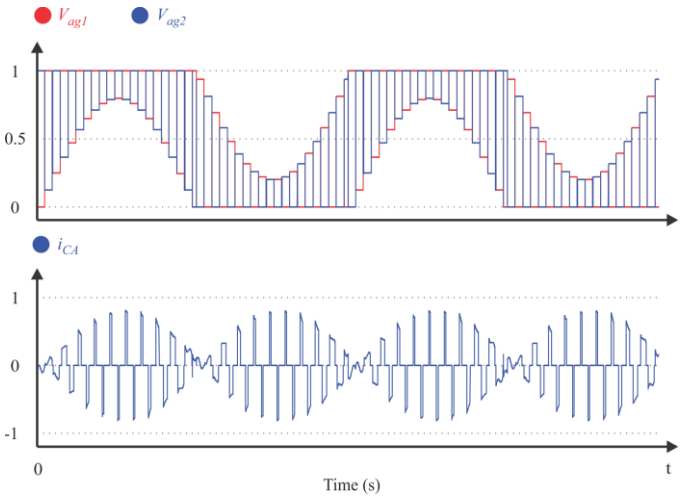

Fig. 5. Changes between the modulating signals using the maximum and minimum values of V_{a_d} and null mean current at high frequency in the capacitor C_a.

Due to the switching between the maximum and minimum values of the voltage V_{a_d}, four possible switching states are obtained. These states are summarized in Table I, as well as the sectors and modulating signals V_{ag1} and V_{ag2}, the voltage V_{a_d}, and the switching states, both for when the carrier reaches its maximum value (Period Match - P) and its minimum value (Underflow - U).

TABLE I
DETAILS OF IMPLEMENTATION OF THE DM MODULATION

Sector	State	V_{ag1}	V_{ag2}	V_{a_d}	Switching State	
					P	U
1	1	PWM	1	R_1	[1 0]	[1 1]
	2	1	PWM	R_2	[0 1]	[1 1]
2	3	0	PWM	R_3	[0 0]	[0 1]
	4	PWM	0	R_4	[0 0]	[1 0]

* adopted of [1].

Figure 6 is an example showing all the possibilities contained in Table I.

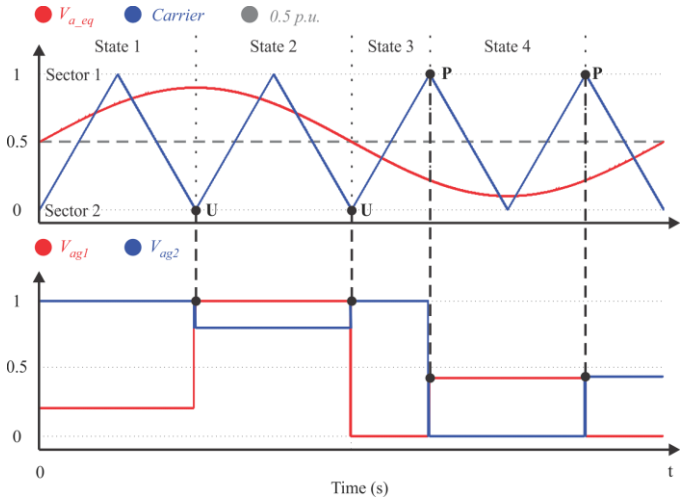

Fig. 6. Modulating voltages switching states in Period Match and Underflow.

Based on Table I and Figure 6, the exact moments in which state transitions occur in Sectors 1 and 2 are observed. In Sector 1, the states are alternating between states 3 and 4, whereas for the Sector 2 they are alternating between states 1 and 2.

III. Simulations Results

Initially, it is necessary to define the operating conditions of the converter. The nominal power is equal to 10 kW and the DC link voltage is equal to 1000 V. The parameters for the converter simulation were defined from these values, summarized in Table II.

TABLE II
PARAMETERS OF IMPLEMENTATION OF THE CONVERTER

Parameter	Value
DC link voltage	1000 V
Nominal power	10 kW
Switching frequency	2.5 k Hz
Flying capacitors (C_a, C_b, C_c)	1.5 mF
Inductive filter	2 mH
Line Voltages	220 V_{rms}
Fundamental frequency	50 Hz
Nominal load	5 Ω
Sampling period	20 µs

To verify the implementation of the PD and PS modulations, the phase and line voltages, as well as the output current and the modulating signals required for the converter operation are initially verified. In both tests, the converter operates at nominal power.

The results for PD modulation are presented in Figure 7, which showed distortions in the waveforms of phase and line voltages of the converter. These distortions are explained due to the variations of voltages in the flying capacitors. In the case of PS modulation implementation, the voltage levels are well defined in three levels in the phase voltages and five levels in the line voltages. Figure 8 shows the result.

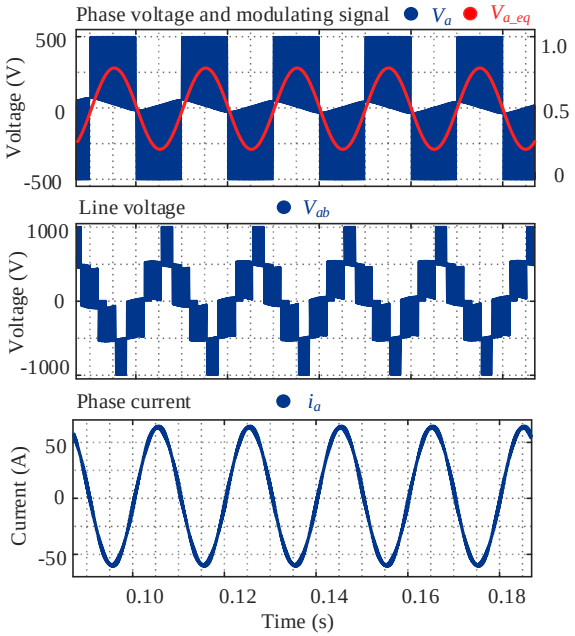

Fig. 7. Results of simulation for PD modulation.

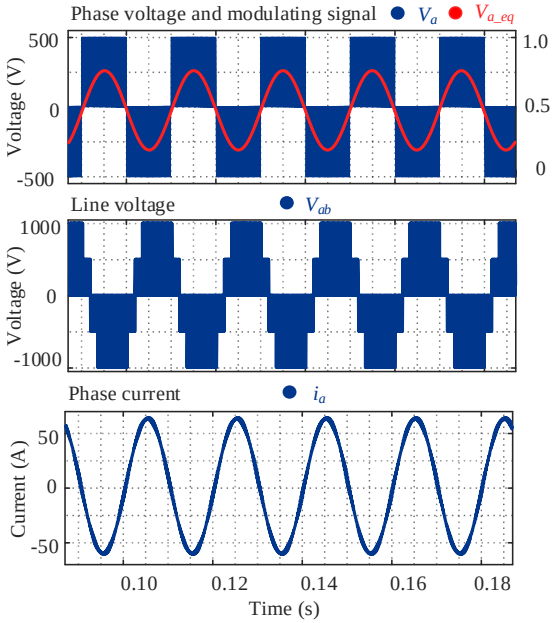

Fig. 8. Results of simulation for PS modulation.

The implementation of the carrier-based DM is shown in Figure 9. In the modulating signals is verified the presence of a third harmonic component, multiple of the fundamental frequency of the output voltage. This is a characteristic of modulations by geometric approaches.

In relation to the converter phase and line voltages, both have characteristics similar to PD modulation. However, in the case of carrier-based DM, the results have three and five levels well defined. It occurs because the currents referring to the flying capacitors have a ripple with high frequency, as previously shown in Figure 5.

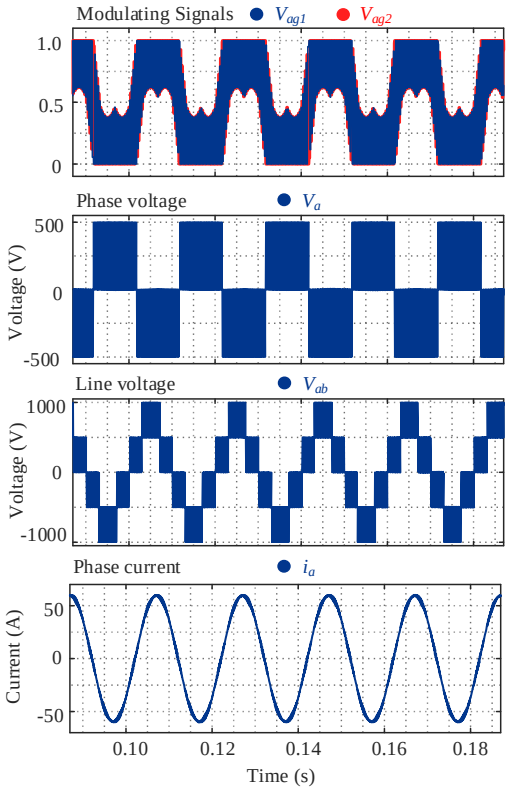

Fig. 9. Results of simulation for PS modulation.

This affirmation can be verified by Figure 10, where the voltages of the flying capacitors of the three modulations are presented. In relation to the PS and DM modulations, it presents low voltage ripple, whereas for the PD modulation the low-frequency current variations of the flying capacitors cause large voltage variations.

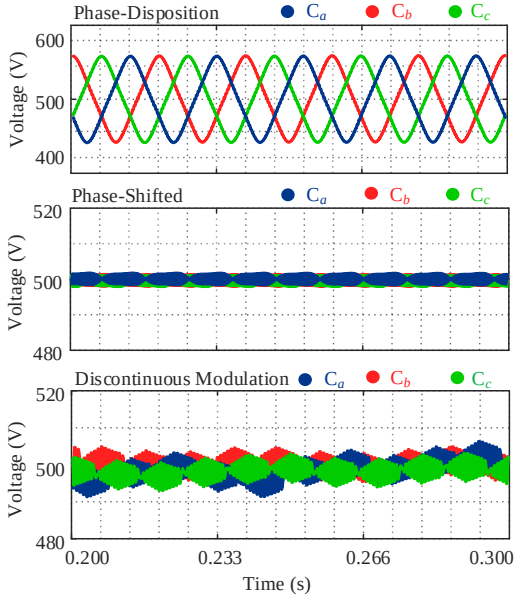

Fig. 10. Voltages of the flying capacitors.

To verify the pulse distribution in the semiconductors, the modulating and carrier signals are analyzed for a specific time interval, which represents 1/8 of the fundamental frequency of the output voltage.

Figure 11-a show the voltage pulses in the semiconductor $\bar{S}_{a1}$ for PD modulation. In this case, it is verified that the distribution of the pulses is not uniform, because the voltage on $\bar{S}_{a1}$ saturates at 500 V during half a cycle of the output voltage. On the other hand, in Figure 11-b it is observed that the pulses are uniformly distributed over time for PS modulation, which can reduce the total harmonic distortion and balance losses between semiconductors. However, the number of switching increases in relation to PD modulation. For carrier-based DM, Figure 11-c shows the pulses distributed (PS) with a reduced number of switching (PD).

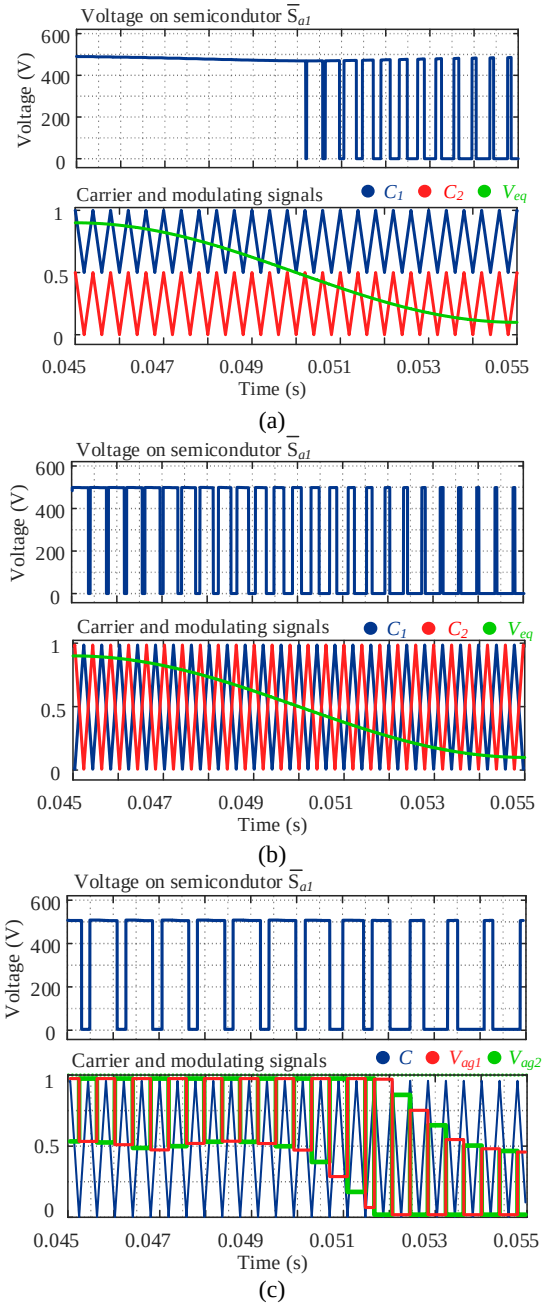

Fig. 11. Pulse distribution of a) PD; b) PS; c) carrier-based DM.

After analyzing the waveforms required to verify the proper operation of the inverter with the different modulations presented, a quantitative comparison of the performance characteristic of the modulations is presented in the sequence of

this paper: a) the number of semiconductor switches per cycle of the fundamental frequency of the output voltage; b) Total harmonic distortion.

In order to carry out this comparison, the converter was initially simulated considering the nominal operating conditions. In relation to the number of switching, it is verified by Figure 12-a that the DM and PD modulations have a reduced number of switching when compared with the PS modulation. This characteristic is interesting because it allows reducing significantly the converter switching losses.

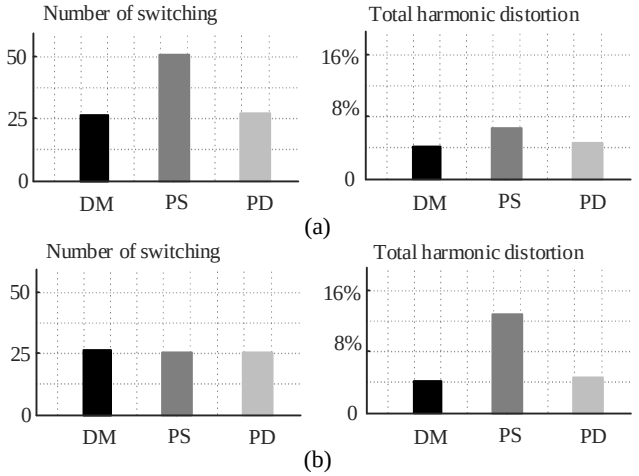

Fig. 12. Comparison of different modulations applied to the FC inverter, considering: a) the same frequency of operation; b) the same number of semiconductor switching;

For the carrier-based DM, 52 commutations were counted during a 50 Hz cycle, number near the 50 commutations of the PD modulation. On the other hand, the PS modulation presented twice as many commutations in relation to the other modulations. Regarding to the total harmonic distortion, according to the graphs presented in Figure 12-a, DM and PD modulations presented better results than the PS modulation. This becomes clear when the switching counts for the three modulations are the same. To achieve this feature, the switching frequency of the PS modulation is reduced, resulting in an even higher THD. Therefore, it can be concluded that the DM modulation combines interesting characteristics of both the PD and PS modulation, these being:

- Low harmonic distortion rate (PD);
- Reduced number of switching (PD);
- Better distribution of semiconductor switching (PS);
- Possibility of reducing flying capacitors values (PS).

IV. Conclusions

This paper presents a comparison of different modulations applied in the operation of multilevel inverters. For this, the PD, PS, and carrier-based DM modulations are implemented through simulations, applied to a three-phase Flying-Capacitor converter. In all the cases presented, different issues were evaluated, as well the number of switching, total harmonic distortion, and balanced voltage of the flying capacitors.

With the characteristics of each modulation, the results obtained and the comparisons criteria show that carrier-based DM presents some advantages over the PD and PS modulations, since it combines characteristics of both, resulting in low levels of harmonic distortion, reduced number of switching, as well maintains balanced voltages on capacitors with low ripple.

Acknowledgments

The authors thank INCTGD, CAPES, CNPq, and FAPERGS for the financial support received for the development of this work. L. Michels were supported by a research grant of CNPq – Brasil. The present work was carried out with the support of the INCTGD and the financing agencies (CNPq process 465640/2014-1, CAPES process No. 23038.000776/2017-54 and FAPERGS 17/2551-0000517-1) and CAPES-PROEX. This study was financed in part by the Coordenação de Aperfeiçoamento de Pessoal de Nível Superior – Brasil (CAPES) – Finance Code 001.

References

[1] A. Nicolini, A. Ricciotti, F. Carnielutti, H. Pinheiro "Carrier-Based Discontinuous Modulation for Inverters With Parallel Legs" Brazilian Power Electronics Journal, Campo Grande, v. 21, n.4, 2016.

[2] K. Sharifabadi, L. Harnefors, H. Nee, S. Norrga, R. Teodorescu "Design, Control, and Application of Modular Multilevel Converters for HVDC Transmission Systems" IEEE Press, J. Wiley & Sons, 2016.

[3] X. Guo , B. Wei, T. Zhu, Z. Lu, L. Tan, X. Sun, C. Zhang "Leakage Current Suppression of Three-Phase Flying Capacitor PV Inverter With New Carrier Modulation and Logic Function" IEEE Transactions On Power Electronics, Vol. 33, No. 3, 2018.

[4] M. M. Silva, A. Toebe, Humberto Pinheiro, "Discontinuos Carrier-Based Modulation For Three Level Flying Capacitor Converter" Brazilian Power Electronics Conference – COBEP, Juiz de Fora, 2017.

[5] H. R. Teymour, D. Sutanto, K. M. Muttaqi, P. Ciufo "A Novel Modulation Technique and a New Balancing Control Strategy for a Single-Phase Five-Level ANPC Converter" IEEE Transactions On Industry Applications, Vol. 51, No. 2, 2015.

[6] G. Gohil, R. Maheshwari, L. Bede, T. Kerekes, R. Teodorescu, M. Liserre, F. Blaabjerg "Modified Discontinuous PWM for Size Reduction of the Circulating Current Filter in Parallel Interleaved Converters" IEEE Transactions on Power Electronics, Vol. 30, No. 7, 2015.

[7] A. A. Abduallah1, M. Meraj, M. Al-Hitmi, A. Iqbal, "Space vector pulse width modulation control techniques for a five-phase quasi-impedance source inverter" IET on Electric Power Application, Vol. 12 Iss. 3, 2018.

[8] L. Gang, W. Dafang, W. Miaoran, Z.Cheng, W. Mingyu, "Neutral-Point Voltage Balancing in Three-Level Inverters Using an Optimized Virtual Space Vector PWM With Reduced Commutations", IEEE Transactions On Industrial Electronics, Vol. 65, No. 9, 2018.

[9] Y. Luo, C. Liu, F. Yu, "Predictive current control of a new three-phase voltage source inverter with phase shift compensation" IET Electric Power Applications, Vol. 11, 2017.

[10] L. Diao , L. Wang, H. Du, L. Wang, Z. Liu, S. M. Sharkh, "AI-HM Based Zero Portion Effects and Phase-Shift Optimization for Railway Auxiliary Inverter With Pulsating DC-Link", IEEE Access, Vol. 5, 2017.

[11] G. Konstantinou , G. Capella , J. Pou, S. Ceballos "Single-Carrier Phase-Disposition PWM Techniques for Multiple Interleaved Voltage-Source Converter Legs" IEEE Transactions On Industrial Electronics, Vol. 65, No. 6, 2018.

[12] B. P. McGrath, C. A. Teixeira, D. G. Holmes, "Optimized Phase Disposition (PD) Modulation of a Modular Multilevel Converter" IEEE Transactions on Industry Applications, Vol. 53, No. 5, 2017.

[13] F. Carnielutti, H. Pinheiro, C. Rech, "Generalized Carrier-Based Modulation Strategy for Cascaded Multilevel Converters Operating Under Fault Conditions" IEEE Transactions On Industrial Electronics, Vol. 59, No. 2, 2012.

[14] G. Carrara, S. Gardella. M. Marchesoni, R. Salutari, G. Sciutto, "A New Multilevel PWM Method: A Theoretical Analysis" IEEE Transactions on Power Electronics, Vol. 7, No. 3, 1992.

[15] D. G. Holmes, T. A. Lipo, "Pulse Width Modulation for Power Converters: Principles and Practice" IEEE Press, J. Wiley & Sons, 2003.